Polymer 50 (2009) 271–278

Contents lists available at ScienceDirect

Polymer

journal homepage: www.elsevier.com/locate/polymer

Phase behavior and structure formation for diblock copolymers composed of side-chain liquid crystalline and glassy amorphous components

Hiroki Takeshita [a], Shin-ichi Taniguchi [a], Mitsuo Arimoto [a], Masamitsu Miya [a], Katsuhiko Takenaka [a,b], Tomoo Shiomi [a,b,*]

[a] Department of Materials Science and Technology, Nagaoka University of Technology, 1603-1 Kamitomioka, Nagaoka, Niigata 940-2188, Japan
[b] Center for Green-Tech Development in Asia, Nagaoka University of Technology, 1603-1 Kamitomioka, Nagaoka, Niigata 940-2188, Japan

ARTICLE INFO

Article history:
Received 22 August 2008
Received in revised form
20 October 2008
Accepted 3 November 2008
Available online 12 November 2008

Keywords:
Liquid crystalline block copolymer
Microphase separation
Time-resolved SAXS

ABSTRACT

Phase behavior and structure formation in liquid crystallization of a side-chain liquid crystalline (LC) block copolymers composed of poly[11-(4′-cyanophenyl-4″-phenoxy)undecyl acrylate] ($PA_{11}OCB$) and polystyrene (PSt) were investigated by using a time-resolved small-angle X-ray scattering technique (SAXS), differential scanning calorimetry and polarizing optical microscopy. $PA_{11}OCB$ homopolymer formed smectic (Sm) liquid crystal. Liquid crystallization behavior of the block copolymers depended on the molecular weight and the block composition. When molecular weight was relatively low, order–disorder transition (ODT) was observed. In cooling of such block copolymers, liquid crystallization seemed to wait for the formation of LC-rich microphase by ODT. For the block copolymers with relatively high molecular weight, liquid crystallization slightly enlarged the domain spacing without changing the microphase separation structure in the melt. The order of the LC phase was lowered with decreasing dimensionality of the LC microdomains, that is, the LC blocks formed smectic liquid crystal in the matrix or lamellar microphase while liquid crystallization in the cylindrical microdomains did not show smectic but maybe nematic liquid crystal. Moreover, the LC blocks within the spherical microdomains did not liquid crystallize. From the 2-D SAXS with applying shear flow, the Sm layers were orientated perpendicularly to the interface of the microphase separation. The relation between the layer thickness of the LC phase and the molecular weight suggested that the main chain was extended normally to the interface of the microphase separation.

1. Introduction

Block copolymers with a crystalline or a liquid crystalline (LC) component have attracted much interest because of their abilities to form hierarchic structure composed of microphase separation, and liquid crystal structure or crystal lamellar structure [1–23]. For crystalline–amorphous block copolymers, crystallization behavior from microphase-separated melt and structural changes of microphase separation by crystallization have been extensively studied [1–6]. In those systems, the main interest has been whether or not crystallization disrupts preexisting microphase separation structure. It has been concluded that the structural changes depend on the competition between crystallization and chain diffusion as well as segregation degrees of microphase separation [3–6]. Besides the structural changes of microphase separation, crystallization behavior within the microdomains has also been discussed for crystalline block copolymers, where it has been revealed that crystallization within small microdomains is strongly obstructed. The obstruction was pronounced especially when the amorphous component is glassy and the crystalline component is in spherical or cylindrical microphases [6,7].

On the other hand, liquid crystalline block copolymer is also attracting increasing interest [8–23]. Using an analogy from crystalline ones, the first interest is whether or not liquid crystallization changes the preexisting microphase separation structure. According to previously reported studies, in the liquid crystalline state, microphase separation structure remains unchanged [13–17]. This is quite different from crystalline block copolymers, in which microphase separation structure can be completely reorganized into crystal lamellar structure [2,3]. Recently we have found the possibility that, in liquid crystalline block copolymers with a rubbery amorphous component, the preexisting microphase separation structure is discontinuously changed by isotropic–smectic phase transition [24]. Structural changes in liquid crystallization of block copolymers have not been fully understood and organized yet. The second interest is liquid crystallization behavior

* Corresponding author. Department of Materials Science and Technology, Nagaoka University of Technology, 1603-1 Kamitomioka, Nagaoka, Niigata 940-2188, Japan. Fax: +81 258 47 9300.
E-mail address: shiomi@vos.nagaokaut.ac.jp (T. Shiomi).

0032-3861/$ – see front matter © 2008 Elsevier Ltd. All rights reserved.
doi:10.1016/j.polymer.2008.11.003

from microphase-separated melt, where it is expected that confinement by microphase separation may influence liquid crystallization behavior. LC transition temperature and transition enthalpy may be lowered because a decrease in order parameter reduces the elastic energy caused by the curvature of interface of microphase separation structure [25]. In addition, orientation direction of mesogenic groups to the interface of microphase separation is also an important interest because of the possibilities for microphase separation structure to control the orientation of mesogens other than surface rubbing of a cell for a LC device.

In this study, structure formation in liquid crystallization of block copolymers composed of side-chain liquid crystalline and glassy amorphous blocks was investigated by means of differential scanning calorimetry (DSC), polarizing optical microscopy (POM) and a time-resolved small-angle X-ray scattering (SAXS) technique employing synchrotron radiation as light source. We will show structural changes in liquid crystallization with comparing to those with rubbery amorphous blocks. The orientation of the mesogenic groups will be also discussed.

2. Experimental section

2.1. Synthesis

Poly[11-(4′-cyanophenyl-4″-phenoxy)undecyl acrylate] ($PA_{11}OCB$) homopolymer and block copolymers composed of $PA_{11}OCB$ and polystyrene (PSt) (Fig. 1) were prepared by atom transfer radical polymerization (ATRP). Synthesis of the liquid crystalline (LC) monomer and the polymerization were carried out according to the method of Kasko et al. [10,12] As a Cu-solubilizing ligand in ATRP, 4,4′-dinonyl-2,2′-dipyridyl (bpy9) was used instead of 4,4′-diheptyl-2,2′-dipyridyl (bpy7) used in the literature. For synthesis of the LC homopolymer, ATRP was performed at 110 °C for 3 h by using 11-(4′-cyanophenyl-4″-phenoxy)undecyl 2-bromopropionate as an initiator. The obtained LC homopolymer was purified by reprecipitating three times with a THF/methanol system to remove unreacted monomer, CuBr and bpy9, followed by drying under vacuum. The block copolymers were synthesized by ATRP of the LC monomer using a PSt macroinitiator, which is also synthesized by ATRP. The polymerization for the PSt macroinitiator was carried out for 1.5 h at 110 °C, and the resulting product was purified by reprecipitation with a THF/hexane system. The block copolymerization of the LC monomer was carried out at 110 °C for 3 h. The obtained block copolymers were purified with a THF/methanol system, followed by drying under vacuum.

Molecular weights of PSt macroinitiators and $PA_{11}OCB$ homopolymers were measured by size exclusion chromatography (SEC) using a TOSOH HLC-8020 instrument equipped with an RI detector. Copolymer compositions of the block copolymers were determined by 400 MHz ^{1}H NMR in $CDCl_3$ with a JEOL JNM-GX400 spectrometer. Molecular weights of the block copolymers were estimated from the copolymer composition on the basis of the molecular weight of PSt macroinitiators. Polydispersity of molecular weights was determined by SEC with the RI detector.

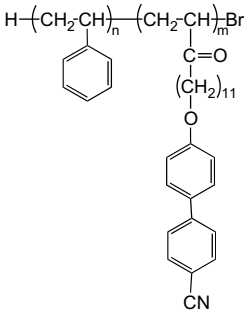

Fig. 1. Chemical structure of $PA_{11}OCB$–PSt.

Characteristics of a $PA_{11}OCB$ homopolymer and the block copolymers are shown in Table 1. The LC phase transition temperatures, transition enthalpies, LC transition behavior and morphology of microphase separation, which will be discussed in the following sections, are also listed in the table.

2.2. Sample preparation and measurements

The polymers were dissolved in THF and then cast from 5 wt% solution to form films, which were dried for three days at room temperature and then under vacuum overnight. The cast films were packed in DSC sample pans and sample cells for SAXS measurements. The SAXS cells had a path length of 1 mm and were sealed with polyimide films.

Structure of microphase separation and liquid crystal was observed by one- and two-dimensional small-angle X-ray scattering techniques (1-D- and 2-D-SAXS). Time-resolved 1-D and 2-D SAXS experiments were performed using synchrotron radiation at beamline BL-10C and BL-15A, respectively, of the Photon Factory at the Institute of Materials Structure Science of the High Energy Accelerator Research Organization in Tsukuba, Japan [26]. Details of the spectrometers were described elsewhere [27,28]. The 1-D-SAXS data were collected in 15 s frames separated by a waiting-time of 5 s using a position sensitive proportional counter (PSPC). For 1-D-SAXS measurements, the sample was first annealed at 140 °C, which is higher than the isotropic–smectic phase transition temperature T_{iso} of the liquid crystalline component, for 30 min, and then cooled down to 40 °C at a rate of 4 °C/min. In the 2D-SAXS experiments, oscillating shear flow was applied to the 100 mm-thick sample at 1 Hz at 80 °C for 20 min using a Linkam CSS-450 apparatus just before SAXS measurements, where the sample was sandwiched between two stainless plates with X-ray windows made of polyimide films. The scattering images in the 2-D experiments were collected by a CCD camera (C4880, Hamamatsu Photonics K.K.) with an image intensifier. The scattering vector was defined as $q = (4\pi/\lambda)\sin(\theta/2)$, where θ and λ are the scattering angle and the wavelength of the X-ray, respectively. The scattering angle was calibrated by a diffraction of a chicken tendon having periodical structure of 65.3 nm.

Morphology of liquid crystalline phase in cooling from the isotropic state was observed by POM under crossed polarizers using an OLYMPUS BH-2 equipped with a digital camera system and a Mettler FP82HT hot stage running through a FP90 central processor. DSC measurements were performed by using a Perkin–Elmer Pyris1 DSC calorimeter calibrated with indium and tin.

Table 1
Characteristics of samples.

Sample	M_n [kg/mol]		w_{LC}[c]	M_w/M_n[a]	Morphology	LC phase transition		
	PSt[a]	PLC[b]				Behavior	T_{iso} [°C]	ΔH [J/g]
S14LC01	14.3	1.4	0.09	1.21	LC sphere	Non	–	–
S09LC04	9.1	4.3	0.22	1.20	LC cylinder	N-Iso	102	4.3
S14LC09	14.3	8.8	0.38	1.12	LAM	Sm-Iso	121	5.9
S09LC13	9.1	13.0	0.59	1.21	PSt cylinder	Sm-Iso	93	4.1
S03LC03	2.6	3.4	0.57	1.18	LAM	N-Iso	78	5.3
S03LC07	2.6	6.7	0.72	1.20	LAM	N-Iso	52	4.8
S03LC25	2.6	24.5	0.88	1.16	PSt sphere	Sm-Iso	126	2.8
LC12	–	12.0	1.00	1.11	–	Sm-Iso	138	7.4

[a] Determined by SEC using standard poly(styrene).
[b] Determined from copolymer composition measured by ^{1}H NMR on the basis of molecular weight of PSt.
[c] Determined by ^{1}H NMR.

3. Results and discussion

3.1. Liquid crystallization behavior of the homopolymer

Figs. 2 and 3 show DSC heating thermograms and POM photographs at 40 °C, respectively, for the homopolymer LC12 and the block copolymers. In LC12, the DSC thermogram shows a transition temperature at 138 °C, below which a birefringent texture specific to liquid crystal is observed in POM. SAXS profiles of the homopolymer are depicted in Fig. 4 for three temperatures. Below the transition temperature, two sharp scattering peaks are observed. The peak positions with a ratio of 1:2 indicate that the homopolymer forms smectic liquid crystal. From the position of the first-order peak ($q^* = 1.44\ \mathrm{nm}^{-1}$ at 79 °C), the spacing of the smectic layers is estimated to be 4.36 nm at 79 °C. T_{iso} and the spacing obtained here is almost the same as those reported by other researchers [10,29]. Because the length of the side-chain of the liquid crystalline polymer is about a half of the spacing, supposing that the methylene spacers between the main chains and the mesogens are stretched to *trans*-zigzag conformation, the smectic layers consist of bilayers as depicted in Fig. 5.

In the inset of Fig. 4, temperature dependence of the position of the first-order peak is shown. The peak position shifts toward lower q with decreasing temperature, which means that the layer spacing becomes larger with lowering temperature. In general, with increasing temperature, the mesogen axis becomes normal against the smectic layer so that the spacing becomes smaller. Although this opposite behavior itself is interesting, it is out of our focus in the present work and remain unclear what kind of structure change enlarges the spacing of the smectic layer.

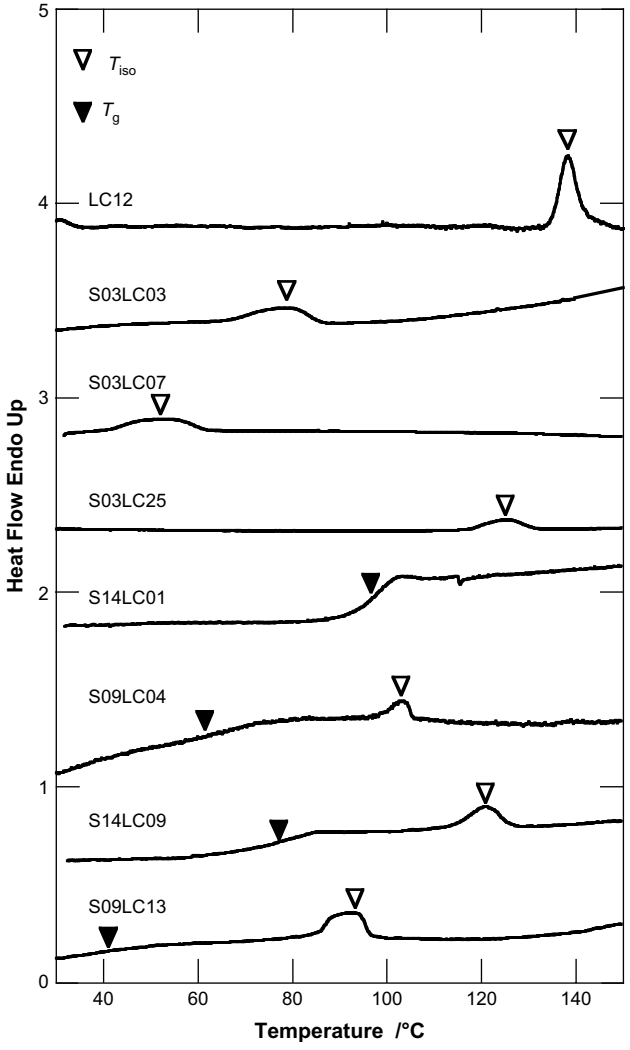

Fig. 2. DSC thermograms in heating at 4 °C/min.

3.2. Mircophase separation and order–disorder transition

In Fig. 6, the SAXS profiles at 25 °C and 140 °C are shown for all of the block copolymers. At 25 °C, which is below T_{iso} of the LC homopolymer, all the SAXS curves have peaks originating from microphase separation structure at around $q = 0.2$–$0.8\ \mathrm{nm}^{-1}$ depending on the molecular weight and the copolymer composition, although the intensity of the scattering peak for S14LC01 is very weak. From the ratio of the higher-order peaks to the first-order one, with taking account of the block composition, S14LC01, S09LC04, S14LC09, S09LC13, S03LC03, S03LC07 and S03LC25 have LC-spherical, LC-cylindrical, lamellar, PSt-cylindrical, lamellar, lamellar and PSt-spherical microphase structures, respectively, which are summarized in Table 1.

At the elevated temperature 140 °C, the block copolymers with a relatively high molecular weight shown in Fig. 6(a) do have scattering peaks from the microphase separation structure at almost the same positions as those at 25 °C, which means that liquid crystallization occurs from ordered melts with preserving the microphase separation structure. On the other hand, as shown in Fig. 6(b), the samples with a relatively low molecular weight do not show any SAXS peaks at 140 °C. This means that they have order–disorder transition (ODT) temperature T_{ODT} between 25 °C and 140 °C, and the relation between T_{iso} and T_{ODT} determines whether liquid crystallization occurs from microphase-separated melt or disordered melt.

Focusing on a higher q range reflecting liquid crystalline structure, some samples have a peak from the smectic structure at about the same position as that for the homopolymer LC12, and the others not. Whether or not a SAXS curve has a peak from smectic liquid crystalline structure seems to depend on the block composition, that is, microphase separation structure. In the following sections, the liquid crystallization behavior will be discussed in two categories, that is, liquid crystallization from microphase-separated melt and from disordered melt.

3.3. Liquid crystallization from microphase-separated melt

As described so far, S14LC01, S09LC04, S14LC09 and S09LC13 seem not to change their microphase separation structure crossing T_{iso}. DSC thermograms and POM photographs at 25 °C for these four samples were depicted in Figs. 2 and 3, respectively. For S09LC13, S14LC09 and S09LC04, LC transition and glass transition of PSt are observed at 85–120 °C and 40–80 °C, respectively. Also in the POM photographs, these three samples show birefringence texture originating from LC phase. However, the SAXS profiles for S09LC13 and S14LC09 are different those for S09LC04. The former two samples show a scattering peak originating from smectic layers at almost the same position as the homopolymer, while the latter does not have any traces of the layered structure although it shows a LC transition in DSC and POM. This means that, LC blocks within matrix or lamellar microphase liquid crystallized in the same manner as the homopolymer, while those within cylindrical microdomains did not. The liquid crystalline structure is not smectic but probably nematic. Moreover, S14LC01 with 9 wt% of the LC component shows only glass transition in the DSC thermogram, and no oriented structure is detected in POM. This means that liquid crystallization was inhibited for S14LC01, in which LC blocks were surrounded by glassy PSt matrix.

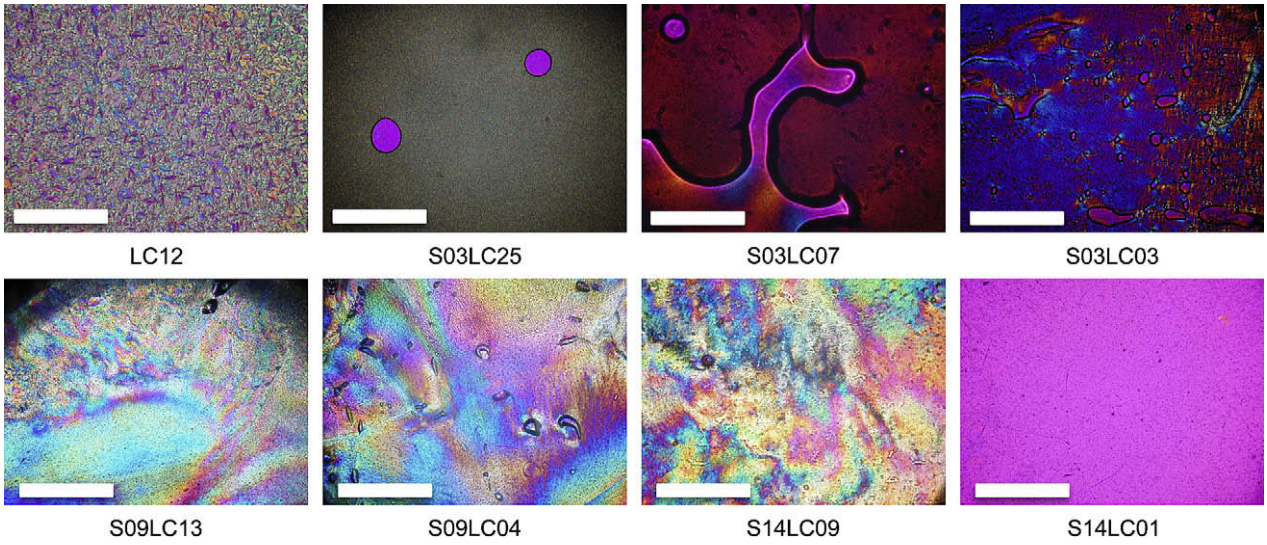

Fig. 3. POM photographs at 40 °C after cooling from 140 °C at a rate of 4 °C/min. The scale bar indicates a distance of 100 μm.

From Fig. 6(a), the positions of the first-order peak at 25 °C for S09LC04 and S14LC01 are $q = 0.32$ and 0.21 nm^{-1}, respectively, although that for S14LC01 may has some margin of error because of its weak peak intensity. From the peak positions, the radii of the cylinders in hexagonal packing and spheres in bcc lattice are 5.6 and 5.3 nm for S09LC04 and S14LC01, respectively, assuming the volume fraction of the components to be the weight fraction. The difference of liquid crystallization behavior between S09LC04 and S14LC01, which have comparable radius of the LC domain, may come from the difference in the dimensionality of the LC domains and the curvature of the interface of microphase separation. We have also studied liquid crystallization of block copolymers composed of the same LC component as studied here and poly(butyl acrylate), in which the amorphous component is rubbery at T_{iso} of the LC blocks, and concluded that liquid crystallization is suppressed within small microdomains even when the surrounding matrix is rubbery [24]. Such kind of the obstruction within small isolated microdomains has been extensively studied for various crystalline–amorphous block copolymers [1–7]. It has been reported that crystallization is strongly suppressed within small isolated microdomains, especially for block copolymers with a glassy amorphous component. The suppression has been attributed to limited growth dimensionality, difficulty of volume change, homogeneous nucleation within isolated domains and so on [6,7]. In addition to such kinds of confinement effects, curvature of interface may be an important factor in liquid crystallization within nanoscale domains.

In Fig. 7, temperature dependence of the position of the first-order peak from microphase separation structure in cooling at 4 °C/min is depicted for S09LC04, S09LC13 and S14LC09. The arrows indicate T_{iso}s determined by DSC. In S09LC13 and S09LC04, q_m becomes smaller at T_{iso}. The reduction in q_m means swelling of the microphase separation structure by liquid crystallization. From the relation, $d = 2\pi/q_m$, the spacings of the microphase separation structure became larger from 24.4 to 26.1 nm and from 19.6 to 20.4 nm for S09LC13 and S09LC04, respectively. The increments correspond to only about 4 and 7% of the spacing in the melt. In

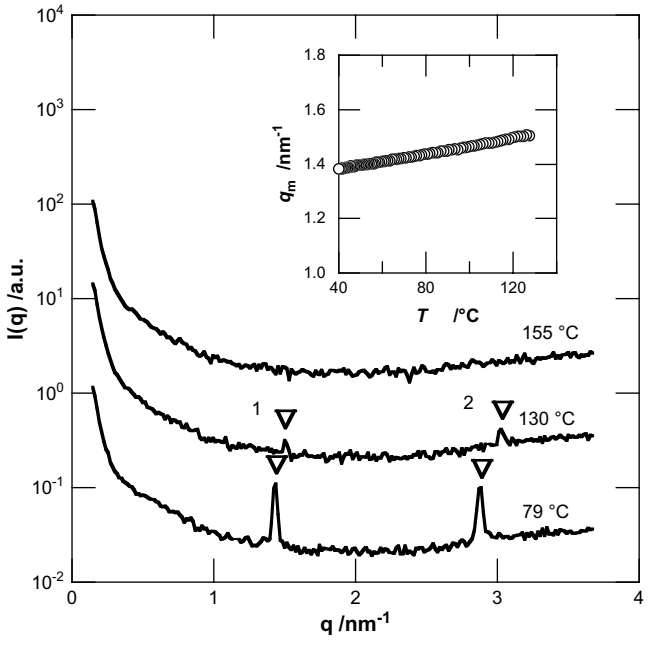

Fig. 4. Temperature dependence of the SAXS profile of LC12. The inset shows the temperature dependence of the position of the first-order peak.

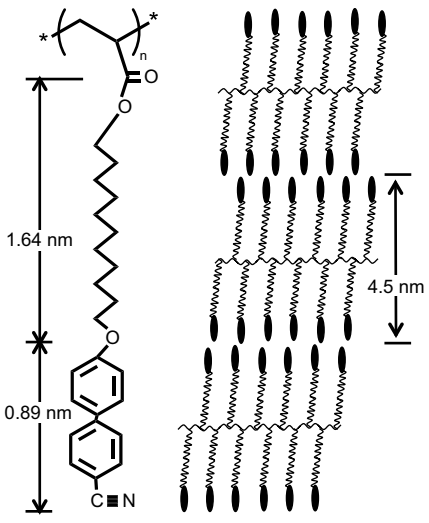

Fig. 5. Schematic representation of the bilayer smectic structure.

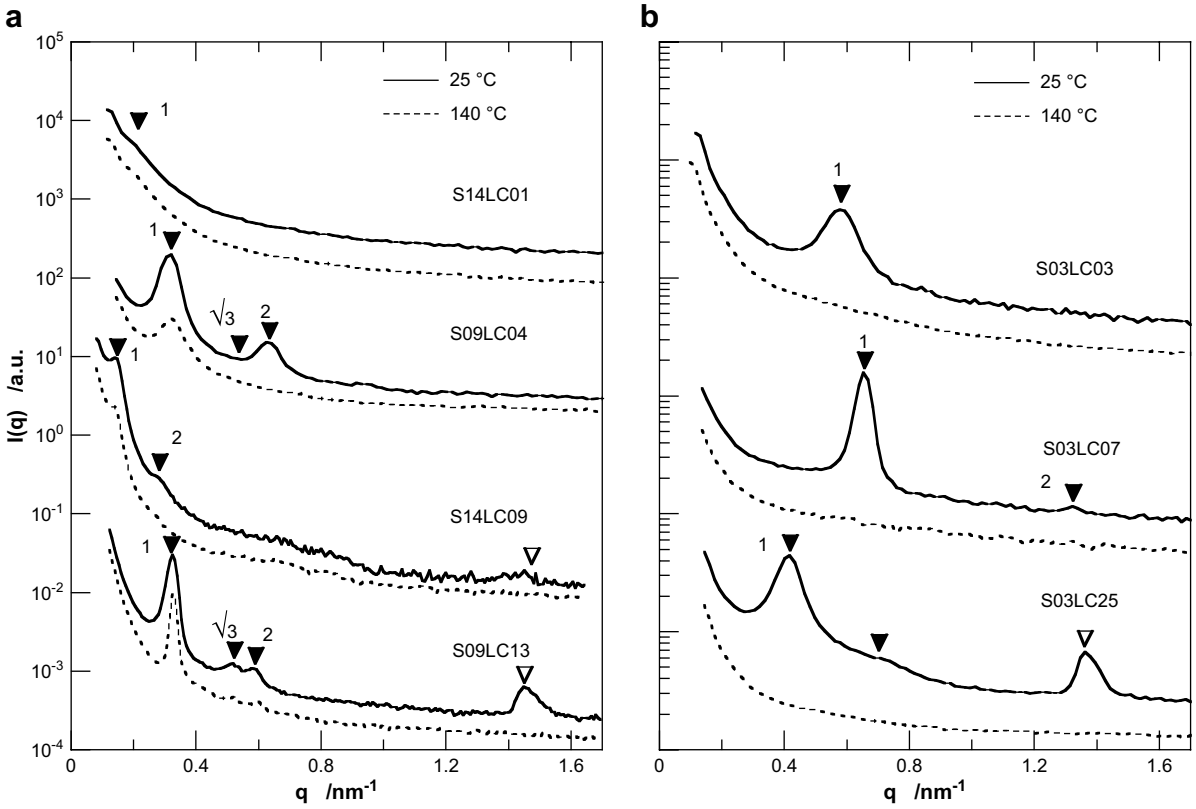

Fig. 6. SAXS profiles in the liquid crystalline and the isotropic state for the block copolymers.

PA_{11}OCB–PBA having a rubbery amorphous component, on the other hand, the domain spacings were enlarged by 15–50% in liquid crystallization, and the highlight was a discontinuous change of the spacings in smectic–isotropic phase transition, that is, a new peak appeared and grew at a lower q while the original peak decreased its intensity and disappeared [24]. Compared with that, the changes in the spacings of PA_{11}OCB–PSt are very small and continuous. This should come from the higher glass transition temperature compared to PA_{11}OCB–PBA. Actually, S14LC09, which has the highest molecular weight of PSt block, does not change its domain spacing in liquid crystallization. The reason why the domain was enlarged by liquid crystallization will be discussed in the later section.

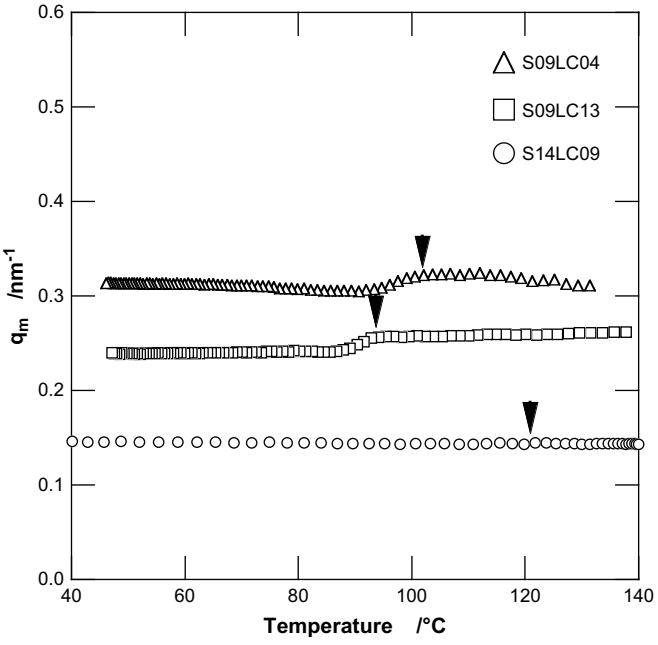

Fig. 7. Temperature dependence of the first-order peak in cooling. The down-pointing arrows indicate T_{iso}s.

3.4. Liquid crystallization from disordered melt

As described before, for the samples with relatively low molecular weight, S03LC03, S03LC07 and S03LC25, no SAXS peak is detected in the melts at 140 °C, while clear peaks are observed at 25 °C (Fig. 6(b)). This means that these show ODT between the two temperatures.

In Fig. 8, temperature dependence of the SAXS profiles in cooling at a rate of 4 °C/min is depicted. With decreasing temperature, all of these have a scattering peak at $q = 0.4$–0.6 nm^{-1}. The peak position q_m and the intensity $I(q_m)$ are plotted against temperature in Fig. 9. T_{iso}s determined by DSC in heating ramp are also indicated by the down-pointing arrows. In S03LC25, T_{iso} is higher than T_{ODT}, meaning that liquid crystallization occurs from disordered melt followed by the formation of microphase separation structure. As S03LC25 contains about 90 wt% of the LC component, it could liquid crystallize from the disordered melt.

For S03LC03 and S03LC07, on the other hand, T_{iso} is almost the same as or lower than T_{ODT}. Although it is hard to find systematic tendency of the relation between T_{iso} and T_{ODT}, T_{iso} is lowered compared to that for the homopolymer. In addition, no SAXS peak originating from Sm phase is also observed in these two samples. This may be the dilution effect due to the relatively low LC weight fractions of 72 and 57 wt% in S03LC07 and S03LC03, respectively. Liquid crystallization might wait for ODT, by which LC-rich phase

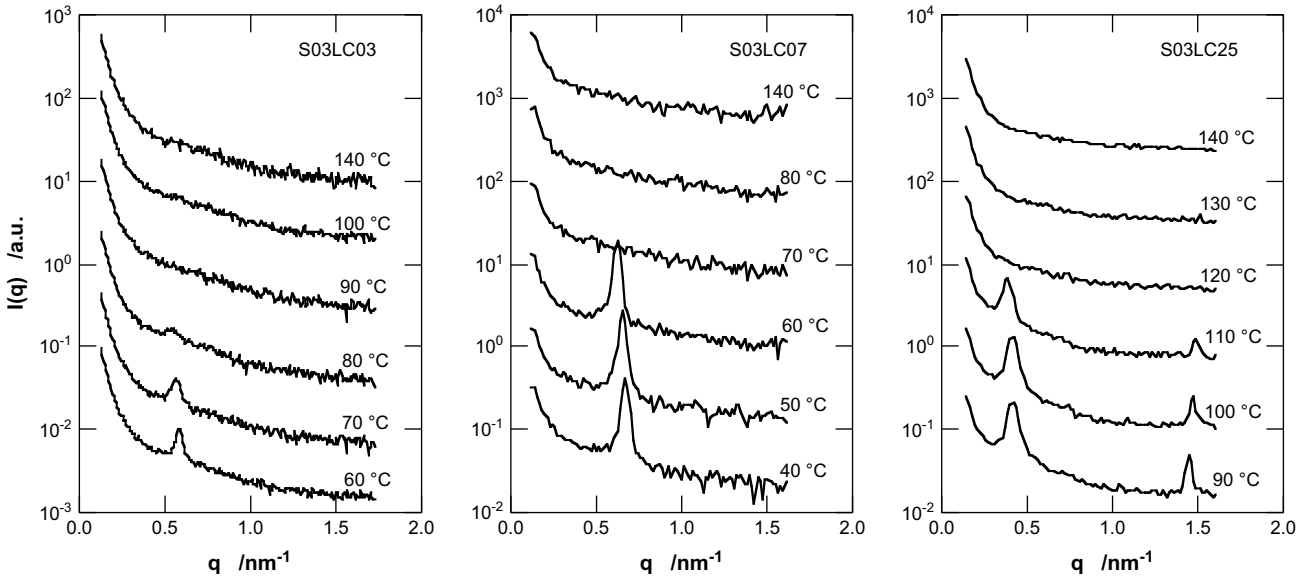

Fig. 8. Temperature dependence of SAXS profiles for S03LC03, S03LC07 and S03LC25 in cooling.

was formed. S03LC03, in which liquid crystallization occurs at almost the same temperature as ODT, may be an example of direct induction of LC transition by ODT. On the other hand, another type of coupling of T_{iso} and T_{ODT} was also reported for other LC block copolymers with relatively low LC composition, where ODT was induced by LC transition [22]. They attributed the induction of ODT to the relief of steric frustration caused by the difference in size between the LC and the amorphous blocks. For S03LC07 and S03LC03, the steric frustration is not so significant compared to their system because they have more than 50 wt% of the LC component. However, it may be necessary to take account of such steric asymmetry between the blocks and other factors for the complete understanding of the suppression of liquid crystallization from disordered melt.

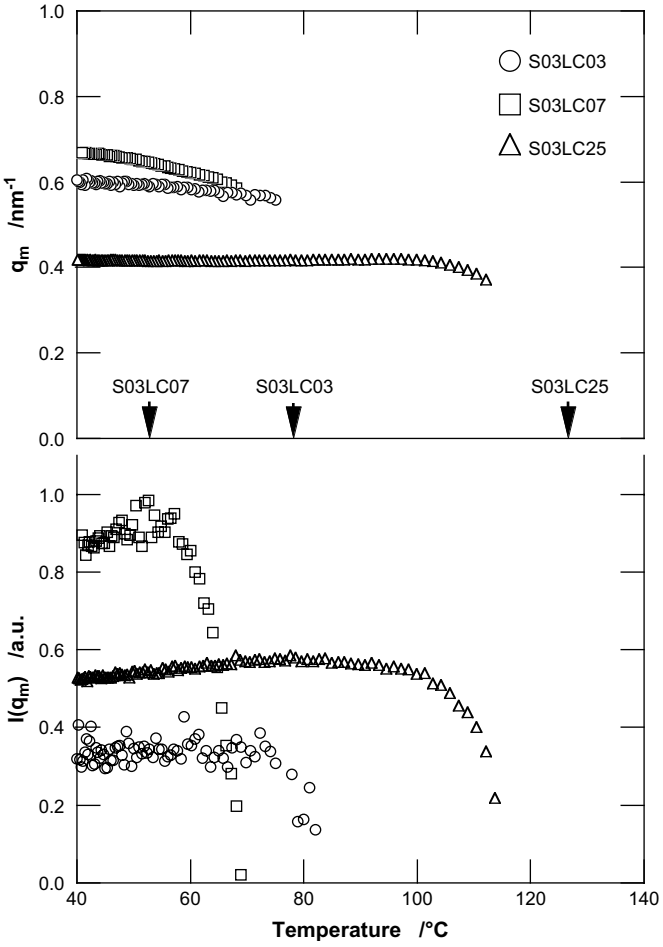

Fig. 9. Temperature dependence of the position and the intensity of the first-order peak. The arrows indicate T_{iso}s determined by DSC in heating ramp.

3.5. LC ordering in microdomains

In this section we focus on the LC structure with spotlighting the orientation direction of the mesogenic groups in the microphase. The direction of the mesogenic groups are evaluated as relation between the interface of the microphase separation structure and the direction of the smectic layers, to which the mesogenic groups are normal in smectic A structure.

In Fig. 10, 2-D-SAXS image after applying shear flow is shown for S09LC13, which has PS-cylindrical microphase separation structure (Fig. 6). The scattering peak from microphase separation is observed at $q = 0.32\ nm^{-1}$. On the other hand, the scattering peaks from the smectic layers at $q = 1.45\ nm^{-1}$ is perpendicularly located to those from the microphase separation. This indicates that the smectic layers are normal to interface of the microphase separation as schematically represented in Fig. 11. The other samples studied here also showed the perpendicular orientation. Also for $PA_{11}OCB$–PBA, we have reported the perpendicular orientation of the smectic layers to the interface.

There are some other studies about the orientation of the mesogenic groups within small microdomains. Anthamatten et al. studied the orientation of smectic layers to microphase separation for roll-cast and fiber-drawn samples and concluded that the direction of the mesogens were governed by the degree of coupling between mesogens and main chains, requirement of splay or bend of smectic layers, conformational changes of main chains, and so on. Specifically, they showed that, in lamellar phase, smectic layers were parallel to the interface for liquid crystalline blocks with a decyl spacer, while perpendicular for those with a hexyl spacer [17]. In LC matrix with PSt cylinders, in addition, they proposed the

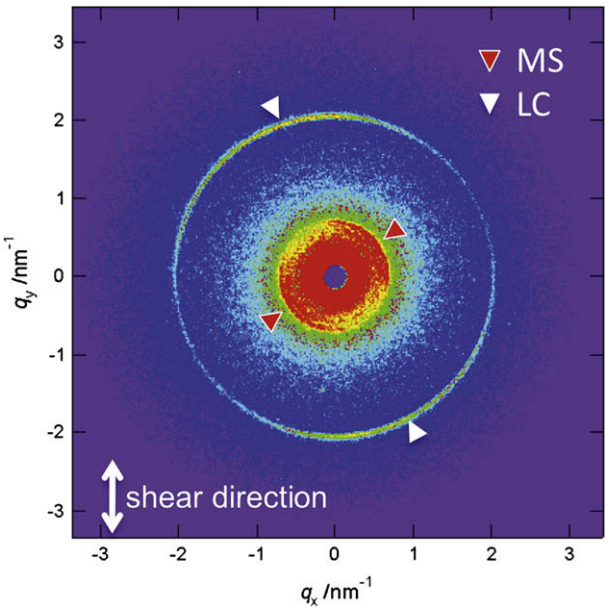

Fig. 10. 2-D-SAXS image for S09LC13 at 80 °C. MS and LC mean microphase separation structure and Sm liquid crystalline structure, respectively.

perpendicular orientation for LC blocks with a hexyl spacer [17,22]. On the other hand, our system in the present and previously reported [24] studies, having an undecyl spacer, shows the perpendicular orientation regardless of the microphase separation structure. Without any coupling between mesogens and interface of microphase separation, smectic layers tend to be parallel to the interface. When mesogens are attached to main chains with long methylene spacers, they should align in the same manner as free mesogens do. Although the liquid crystalline blocks used in the present study have relatively long methylene spacers, the smectic layers align perpendicularly to the interface. This suggests that some other factors such as length and conformation of main chains should be taken into account. At this stage, factors determining the alignment of mesogens remain unclear. More experimental data are required for systematic clarification of the alignment within microdomains.

In perpendicular orientation in liquid crystalline state, the LC main chains must be extended normally to the interface of the microphase separation as schematically shown in Fig. 11. This may be the reason why the domain spacings of the microphase separation became larger in liquid crystallization (Fig. 7). In fact, the stretched main chain in LC state can be confirmed by the absolute values of the domain size. Supposing that the lamellar thickness of

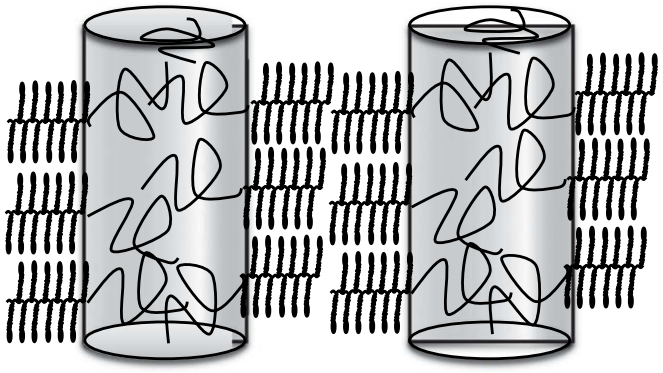

Fig. 11. Schematic model of the phase structure in liquid crystalline state.

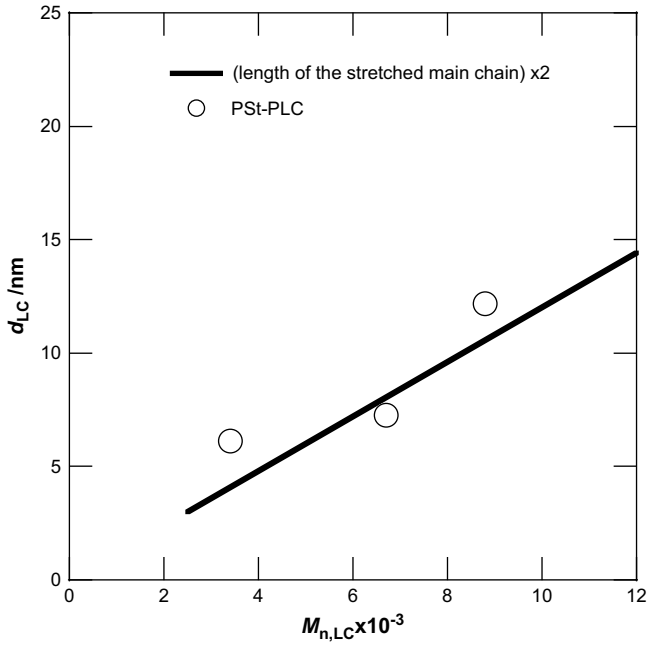

Fig. 12. Dependence of the domain thickness of the LC phase d_{LC} on the molecular weight of the LC block $M_{n,LC}$. The solid line indicates the twice the end-to-end distance of the fully extended LC main chain.

the LC and the amorphous phase is proportional to the copolymer composition, the lamellar thickness of the LC phase, d_{LC}, can be estimated for S14LC09, S03LC03 and S03LC07, all of which form lamellar microphase separation. In Fig. 12, d_{LC} is plotted against M_n of LC blocks. They are almost on the solid line representing twice the end-to-end distance of the fully extended LC main chain with the corresponding molecular weight, which is calculated on the basis of 0.254 nm of C–C–C length per monomer. This linear relationship between d_{LC} and M_n suggests that the LC blocks are stretched and normal to the interface of the microphase separation. These results coincide with the orientation of the smectic layers to the interface of microphase separation.

4. Conclusion

Phase behavior and structure formation in liquid crystallization of side-chain liquid crystalline–glassy amorphous block copolymers were investigated by means of DSC, POM and SAXS.

For the block copolymers with relatively high molecular weight, liquid crystallization did not change the microphase separation in the melt. The order of the liquid crystalline phase was lowered with decreasing dimensionality of LC phase, that is, the LC blocks formed smectic liquid crystal in the matrix of lamellar microphase while liquid crystallization in the cylindrical microdomains did not show smectic but may be nematic liquid crystal. Moreover, the LC blocks within the spherical domains did not liquid crystallize.

Those with relatively low molecular weight had T_{ODT} in the temperature range of observation. In cooling of the samples with relatively low LC composition, liquid crystallization seemed to wait for the formation of LC-rich phase by microphase separation.

The relation between directions of the orientation of microphase separation and Sm layers was measured by 2-D SAXS under shear flow. The Sm layers were perpendicular to the interface of the microphase separation. From the layer thickness of LC phase, it was suggested that the main chain was extended normally to the interface of the microphase separation. This result is different from previously reported one [22], where LC blocks with more than six

methylene units as a spacer between the mesogen and the backbone showed parallel orientation.

Acknowledgements

This work was supported by Grants-in-Aid for Scientific Research on Basic Areas (B) (18350114) from Japan Society for the Promotion of Science and by the 21st Century COE Program for Scientific Research from the ministry of Education, Culture, Sports, Science and Technology. The SAXS experiments using synchrotron radiation were performed under the approval of the Photon Factory Program Advisory Committee (Proposal 2007G090 and 2008G066).

References

[1] Hamley IW. The physics of block copolymers. New York: Oxford; 1998 [Chapter 5].
[2] Muller AJ, Balsamo V, Arnal ML. Adv Polym Sci 2005;190:1–63.
[3] Shiomi T, Tsukada H, Takeshita H, Takenaka K, Tezuka Y. Polymer 2001; 42:4997.
[4] Hamley IW, Fairclough JPA, Terrill NJ, Ryan AJ, Lipic PM, Bates FS, et al. Macromolecules 1996;29:8835.
[5] Liu LZ, Yeh F, Chu B. Macromolecules 1996;29:5336.
[6] Takeshita H, Ishii N, Araki C, Miya M, Takanaka K, Shiomi T. J Polym Sci Part B Polym Phys 2004;42:4199.
[7] Loo Y-L, Register RA, Ryan AJ. Macromolecules 2001;34:8968–77.
[8] Fischer H, Poser S, Arnold M, Frank W. Macromolecules 1994;27:7133–8.
[9] Wang J, Mao G, Ober CK, Kramer EJ. Macromolecules 1997;30:1906–14.
[10] Kasko AM, Heinz AM, Pugh C. Macromolecules 1998;31:256–71.
[11] Anthamatten M, Wu JS, Hammond PT. Macromolecules 2001;34:8574–9.
[12] Kasko AM, Grunwald SR, Pugh C. Macromolecules 2002;35:5466–74.
[13] Hamley IW, Castelletto V, Parras P, Lu ZB, Imrie CT, Itoh T. Soft Matter 2005;1:355–63.
[14] Mao G, Wang J, Clingman SR, Ober CK, Chen JT, Thomas EL. Macromolecules 1997;30:2556–67.
[15] Zheng WY, Albalak RJ, Hammond PT. Macromolecules 1998;31:2686–9.
[16] Ansari IA, Castelletto V, Mykhaylyk T, Hamley IW, Lu ZB, Itoh T, et al. Macromolecules 2003;36:8898–901.
[17] Anthamatten M, Zheng WY, Hammond PT. Macromolecules 1999;32:4838–48.
[18] Yamada M, Itoh T, Nakagawa R, Hirao A, Nakahama S, Watanabe J. Macromolecules 1999;32:282–9.
[19] Li MH, Keller P, Albouy PA. Macromolecules 2003;36:2284–92.
[20] Hamley IW, Castelletto V, Lu ZB, Imrie CT, Itoh T, Al-Hussein M. Macromolecules 2004;37:4798–807.
[21] Tomikawa N, Lu Z, Itoh T, Imrie CT, Adachi M, Tokita M, et al. Jpn J Appl Phys 2005;44:711–4.
[22] Anthamatten M, Hammond PT. Macromolecules 1999;32:8066–76.
[23] Al-Hussein M, Séréro Y, Konovalov O, Mourran A, Möller M, de Jeu WH. Macromolecules 2005;38:9610–6.
[24] Taniguchi S, Takeshita H, Arimoto M, Miya M, Takenaka K, Shiomi T. Polymer, 2008;49:4889–98.
[25] Wen B, Kim JH, Yokoyama H, Rosenblatt C. Phys Rev E 2002;66:041502.
[26] http://pfwww.kek.jp/.
[27] Ueki T, Hiiragi Y, Kataoka M, Inoko Y, Amemiya Y, Izumi Y, et al. Biophys Chem 1985;23:115–24.
[28] Amemiya Y, Wakabayashi K, Hamanaka T, Wakabayashi T, Matsushita T, Hashizume H. Nucl Instrum Methods 1983;208:471–7.
[29] Kostromin SG, Shibaev VP. Polym Sci Ser B 1999;41:346–58.